Published for SISSA by Springer
Received: March 13, 2014
Revised: April 23, 2014
Accepted: April 23, 2014
Published: May 20, 2014

Higgsphobic and fermiophobic Z' as a single dark matter candidate

Nan Chen,[a] **Ying Zhang,**[b] **Qing Wang,**[a,c,d,1] **Giacomo Cacciapaglia,**[e,f,1] **Aldo Deandrea**[e,f,g] **and Luca Panizzi**[h]

[a] *Department of Physics, Tsinghua University, Beijing 100084, P.R. China*
[b] *School of Science, Xi'an Jiaotong University, Xi'an 710049, P.R. China*
[c] *Center for High Energy Physics, Tsinghua University, Beijing 100084, P.R. China*
[d] *Collaborative Innovation Center of Quantum Matter, Beijing 100084, P.R. China*
[e] *Université de Lyon, F-69622 Lyon, France*
[f] *Université Lyon 1, Villeurbanne, CNRS/IN2P3, UMR5822, Institut de Physique Nucléaire de Lyon, F-69622 Villeurbanne Cedex, France*
[g] *Institut Universitaire de France, 103 boulevard Saint-Michel, 75005 Paris, France*
[h] *School of Physics and Astronomy, University of Southampton, Highfield, Southampton SO17 1BJ, U.K.*

E-mail: chen-n08@mails.tsinghua.edu.cn, hepzhy@mail.xjtu.edu.cn, wangq@mail.tsinghua.edu.cn, g.cacciapaglia@ipnl.in2p3.fr, deandrea@ipnl.in2p3.fr, l.panizzi@soton.ac.uk

Abstract: A spin-1 Z' particle as a single dark matter candidate is investigated by assuming that it does not directly couple to the Higgs boson and standard model fermions and does not mix with the photon and Z boson. The remaining dominant vertices are quartic $Z'Z'ZZ$ and $Z'Z'W^+W^-$, which can induce effective $Z'Z'q\bar{q}$ couplings through standard-model gauge-boson loops. We discuss constraints from the cosmological thermal relic density, and direct and indirect-detection experiments, and find that a dark Z' can only exist above the W boson mass threshold, and the effective quartic coupling of $Z'Z'VV$ is bounded in the region of $10^{-3} \sim 10^{-2}$.

Keywords: Beyond Standard Model, Cosmology of Theories beyond the SM

ArXiv ePrint: 1403.2918

[1] Corresponding author.

doi:10.1007/JHEP05(2014)088

Contents

1 Introduction

After the discovery of the 125 GeV Higgs boson, the standard model (SM) of particle physics has become a complete theory; within the SM, the remaining task is the precision measurements of various Higgs properties, in particular its couplings, and to further narrow down the possible parameter space of new physics. Although the hierarchy and meta-stable vacuum problems remain for the SM Higgs theoretically, for new physics beyond the SM the absence of new physics signals at the LHC to date implies that extensions of the SM still only need to rely on the traditional particle physics facts of non-zero neutrino masses and baryon asymmetry. Given these circumstances, the presence of dark matter (DM) in our Universe becomes an even more important leading empirical evidence for the existence of new physics, because no SM particle can account for DM. Cosmology and astrophysics tell us that almost 85% of matter in our universe is dark, i.e., neutral, non-luminous and non-baryonic. The fact that the abundance of DM is comparable to that of ordinary visible matter seems to imply that DM may have the same or similar origins and properties as ordinary matter. If we accept the conclusion of quantum field theory (QFT) that all matter should be made of particles, then an unambiguous, non-gravitational signal of DM must appear in particle physics experiments. This has driven the particle physics community to try harder to unravel DM's still enigmatic properties.

JHEP05(2014)088

Because details of the particle properties of DM are lacking, the best investigative strategy for theorists is to try to cover as much ground as possible. Considering that QFT classifies particles according to their spin (even or odd half-integers), elementary particles discovered so far all have low spins. Most DM candidates discussed so far in the literature have been assumed to be spin-0 scalars [1–7] or spin-1/2 spinors [8, 9] (for spin-1/2 DM, there are so many papers, here we only cite two effective field analysis papers). Whereas a scalar DM has relatively simple structure and provides possible intimate interplay with the 125 GeV Higgs, a spinor DM extends the traditional observation that matter is composed of spin-1/2 particles. The heavy sterile neutrinos [10] and the lightest neutralino [11] in supersymmetric models are DM candidates belonging to this type. Apart from scalar and spinor DM, the next level of higher-spin candidate particles comprise spin-1 vectors. If we limit ourselves to the simplest vector particle scenario in particle physics, a single extra neutral vector particle, usually denoted by Z', is sufficient. We shall discuss this possibility in the present paper. A higher spin case, spin-3/2 DM, has been discussed in ref. [12].

A vector particle Z' can be viewed as a gauge boson that mediates an extra U(1) gauge force beyond the conventional SM strong $SU(3)_c$ force and electroweak $SU(2)_L \otimes U(1)_Y$ forces. For as yet unknown reasons, this additional U(1) gauge symmetry is spontaneously broken, thus yielding a massive Z'. SM plus Z' is a minimal and well motivated generalisation of the SM; many new-physics models have such a Z' boson (for details see review refs. [13–16]) as a necessary constituent and remnant for new-physics interactions. Before July 4, 2012, the Higgs was the superstar of particle physics searches and a Z' only played a supporting role. With the discovery of the 125 GeV Higgs, a Z' now becomes one of the hot new-physics candidate particles and the LHC is actively searching for it in various channels, with the model-dependent lower mass bound already reaching the TeV-energy region depending on the final state it is assumed to decay into. Now, if we further take the Z' as a DM candidate thus changing the Z' from visible to invisible, the interactions between the invisible Z' and SM particles will be strongly reduced, and the corresponding search strategies (such as direct detection, indirect detection, and collider experiment) will change with respect to those for visible Z'. Various constraints must therefore be re-examined.

In the literature, the invisible Z' has been intensively discussed as a messenger between the visible sector (which contains the SM particles) and a hidden sector (to which DM belongs) [17–28]: in such a scenario, the SM particles can be either charged under the additional gauge symmetry or not. In the event that SM particles are neutral with respect to the extra U(1) symmetry, the interaction occurs via effective operators connecting directly Z' to the SM sector. The simplest case is the kinetic mixing terms between the SM hypercharge field strength and the new Abelian field strength [29]. The underlying reason in adopting Z' as a portal to the hidden sector stems from the traditional mediating role of gauge bosons. In this type of DM models, there are too many unknowns concerning the hidden sector, a situation that is not helpful in DM searches. In this paper, we consider an alternative simple approach by ignoring the conventional messenger role of Z', and instead treat it as pure matter. This approach is similar to the minimal darkon model [1–6] where SM is minimally expanded with the addition of a dark scalar (SM+D), except now we replace the scalar darkon D with a single vector DM candidate Z'. The change from the

JHEP05(2014)088

traditional Z' portal model to our present single dark Z' approach is similar to that from the Higgs portal model (where a scalar is taken as a messenger between the visible and hidden sectors) [30, 31] to the darkon model. After the reduction, because of the unique choice of DM candidate, we can ignore the uncertainties arising from the arbitrary hidden sector in the traditional Z' or Higgs portal models. The difference in the present approach with respect to scalar DM is that our dark Z' is a vector particle, which behaves not like a scalar or Higgs boson, but very much like a Z boson of SM and will have relatively complex interaction structure owing to its polarisation. A spin-1 dark matter candidate appears in models with one extra dimensions [32] and has been widely studied in this context [33, 34]. Note that this is not a generic prediction of extra dimensions, as in higher then 5 dimensions the candidate is a scalar [35–37], and a scalar is again found in models of pseudo-Goldstone Higgs in warped space [38] and technicolor [39].

This paper is organised as follows. In section II, in terms of the model-independent extended electroweak chiral Lagrangian and the six assumptions needed to keep Z' dark, we determine the necessary operators that couple our dark Z' to SM particles. In section III, we calculate the relic density produced from our single dark Z', derive a constraint on the effective coupling of the dark Z' pair to W or Z pairs. Section IV looks at the direct-detection constraint, where we compute the SM gauge-boson-loop-induced $Z'Z'\bar{q}q$ vertex and discuss direct detection. Section V examines indirect-detection constraints and includes discussions of the Pamela, AMS02, and FermiLAT experiments. In section VI, we discuss the combined results and some other possible DM related issues. Section VII presents a summary. Some necessary results for section II are to be found in appendix A.

2 $\mathrm{SU}(2)_L \otimes \mathrm{U}(1)_Y \otimes \mathrm{U}(1)$ theory and Z' as a DM candidate

To make our investigation general, we start from a model-independent effective extended electroweak chiral Lagrangian (EEWCL) proposed in ref. [40],

$$\mathcal{L}_{\mathrm{EEWCL}} = \mathcal{L}_2 + \mathcal{L}_4 + \cdots , \tag{2.1}$$

where $\mathcal{L}_{2n}$ for $n = 1, 2, 3, \ldots$ is the p^{2n}-order of EEWCL with Z' and all SM gauge fields, plus four necessary Goldstone bosons described by a two-by-two unitary matrix field $\hat{U}$. The symmetry of the Lagrangian is $\mathrm{SU}(2)_L \otimes \mathrm{U}(1)_Y \otimes \mathrm{U}(1)$, which will be spontaneously broken to $\mathrm{U}(1)_{\mathrm{em}}$. The SM Higgs field and the fermion fields are not included in the above Lagrangian: in fact, couplings to the Higgs are not required by the symmetry of the model and, if present, would reproduce a model of Higgs portal DM. This implies that we ignore the possible direct (or tree-order) couplings between Z' and Higgs (a dark Z' with direct coupling to the Higgs has been discussed in ref. [41]) or between Z' and SM fermions (a dark Z' coupling directly to SM fermions has been discussed in ref. [42]). These are the first two assumptions we adopt for our dark Z'. These higgsphobic and fermiophobic dark Z' assumptions simplify our theory significantly, and we take it as the first step in our investigation. Although at tree level we can ignore the explicit Higgs and fermion couplings, loops can still induce effective couplings. We shall carefully discuss these loops in section IV.

JHEP05(2014)088

The p^2-order Lagrangian $\mathcal{L}_2$ is [40]

$$\mathcal{L}_2 = -\frac{1}{4}f^2\mathrm{tr}[\hat{V}_\mu\hat{V}^\mu] + \frac{1}{4}\beta_1 f^2\mathrm{tr}[T\hat{V}_\mu]\mathrm{tr}[T\hat{V}^\mu] + \frac{1}{4}\beta_2 f^2\mathrm{tr}[\hat{V}_\mu]\mathrm{tr}[T\hat{V}^\mu] + \frac{1}{4}\beta_3 f^2\mathrm{tr}[\hat{V}_\mu]\mathrm{tr}[\hat{V}^\mu], \tag{2.2}$$

where $T \equiv \hat{U}\tau_3\hat{U}^\dagger$, $\hat{V}_\mu \equiv (D_\mu\hat{U})\hat{U}^\dagger$, and τ_3 is the Pauli matrix. The covariant derivative is

$$D_\mu\hat{U} = \partial_\mu\hat{U} + igW_\mu\hat{U} - i\hat{U}\frac{\tau_3}{2}g'B_\mu - i\hat{U}(\tilde{g}'B_\mu + g''X_\mu)I, \tag{2.3}$$

where $W_\mu \equiv \frac{\tau_i}{2}W_\mu^i$, B_μ, and X_μ are the $\mathrm{SU}(2)_L$, $\mathrm{U}(1)_Y$, and $\mathrm{U}(1)$ gauge fields, respectively, and g, g', g'' are the corresponding coupling constants; $\tilde{g}'$ is a special Stueckelberg coupling. W_μ, B_μ, and X_μ are gauge eigenstates, and the Z' discussed in this paper is the physical state after diagonalization. In $\mathcal{L}_2$, β_1 and β_2 are mass mixing parameters.

The p^4-order Lagrangian $\mathcal{L}_4$ is composed of three terms [40]

$$\mathcal{L}_4 = \mathcal{L}_K + \mathcal{L}_B + \mathcal{L}_A, \tag{2.4}$$

for which the kinetic term $\mathcal{L}_K$ is

$$\mathcal{L}_K = -\frac{1}{4}B_{\mu\nu}B^{\mu\nu} - \frac{1}{2}\mathrm{tr}[W_{\mu\nu}W^{\mu\nu}] - \frac{1}{4}X_{\mu\nu}X^{\mu\nu}. \tag{2.5}$$

The normal term $\mathcal{L}_B$ is

$$\begin{aligned}
\mathcal{L}_B = {} & \frac{1}{2}\alpha_1 gg'B_{\mu\nu}\mathrm{tr}[TW^{\mu\nu}] + \frac{i}{2}\alpha_2 g'B_{\mu\nu}\mathrm{tr}[T[\hat{V}^\mu,\hat{V}^\nu]] + i\alpha_3 g\mathrm{tr}[W^{\mu\nu}[\hat{V}^\mu,\hat{V}^\nu]] \\
& + \alpha_4\mathrm{tr}[\hat{V}_\mu\hat{V}_\nu]\mathrm{tr}[\hat{V}^\mu\hat{V}^\nu] + \alpha_5\mathrm{tr}[\hat{V}_\mu\hat{V}^\mu]\mathrm{tr}[\hat{V}^\nu\hat{V}_\nu] + \alpha_6\mathrm{tr}[\hat{V}_\mu\hat{V}_\nu]\mathrm{tr}[T\hat{V}^\mu]\mathrm{tr}[T\hat{V}^\nu] \\
& + \alpha_7\mathrm{tr}[\hat{V}_\mu\hat{V}^\mu]\mathrm{tr}[T\hat{V}_\nu]\mathrm{tr}[T\hat{V}^\nu] + \frac{1}{4}\alpha_8 g^2\mathrm{tr}[TW_{\mu\nu}]\mathrm{tr}[TW^{\mu\nu}] + \frac{i}{2}\alpha_9 g\mathrm{tr}[TW^{\mu\nu}]\mathrm{tr}[T[\hat{V}_\mu,\hat{V}_\nu]] \\
& + \frac{1}{2}\alpha_{10}\mathrm{tr}[T\hat{V}^\mu]\mathrm{tr}[T\hat{V}^\nu]\mathrm{tr}[T\hat{V}_\mu]\mathrm{tr}[T\hat{V}_\nu] + \alpha_{11}g\epsilon^{\mu\nu\rho\lambda}\mathrm{tr}[T\hat{V}_\mu]\mathrm{tr}[\hat{V}_\nu W_{\rho\lambda}] \\
& + \alpha_{12}g\mathrm{tr}[T\hat{V}^\mu]\mathrm{tr}[\hat{V}^\nu W_{\mu\nu}] + \alpha_{13}gg'\epsilon^{\mu\nu\rho\lambda}B_{\mu\nu}\mathrm{tr}[TW_{\rho\lambda}] + \alpha_{14}g^2\epsilon^{\mu\nu\rho\lambda}\mathrm{tr}[TW_{\mu\nu}]\mathrm{tr}[TW_{\rho\lambda}] \\
& + \alpha_{15}\mathrm{tr}[\hat{V}_\mu]\mathrm{tr}[T\hat{V}^\mu]\mathrm{tr}[T\hat{V}_\nu]\mathrm{tr}[T\hat{V}^\nu] + \alpha_{16}\mathrm{tr}[\hat{V}_\mu]\mathrm{tr}[T\hat{V}^\mu]\mathrm{tr}[\hat{V}_\nu\hat{V}^\nu] + \alpha_{17}\mathrm{tr}[\hat{V}_\mu]\mathrm{tr}[T\hat{V}_\nu]\mathrm{tr}[\hat{V}^\mu\hat{V}^\nu] \\
& + \alpha_{18}\mathrm{tr}[\hat{V}_\mu]\mathrm{tr}[\hat{V}_\nu]\mathrm{tr}[T\hat{V}^\mu]\mathrm{tr}[T\hat{V}^\nu] + \alpha_{19}\mathrm{tr}[\hat{V}_\mu]\mathrm{tr}[\hat{V}_\nu]\mathrm{tr}[\hat{V}^\mu\hat{V}^\nu] + \alpha_{20}\mathrm{tr}[\hat{V}_\mu]\mathrm{tr}[\hat{V}^\mu]\mathrm{tr}[T\hat{V}_\nu]\mathrm{tr}[T\hat{V}^\nu] \\
& + \alpha_{21}\mathrm{tr}[\hat{V}_\mu]\mathrm{tr}[\hat{V}^\mu]\mathrm{tr}[\hat{V}_\nu\hat{V}^\nu] + \alpha_{22}\mathrm{tr}[\hat{V}_\mu]\mathrm{tr}[\hat{V}^\mu]\mathrm{tr}[\hat{V}_\nu]\mathrm{tr}[T\hat{V}^\nu] + \alpha_{23}\mathrm{tr}[\hat{V}_\mu]\mathrm{tr}[\hat{V}_\nu]\mathrm{tr}[\hat{V}^\mu]\mathrm{tr}[\hat{V}^\nu] \\
& + gg''\alpha_{24}X_{\mu\nu}\mathrm{tr}[TW^{\mu\nu}] + g'g''\alpha_{25}B_{\mu\nu}X^{\mu\nu} + \alpha_{26}\epsilon^{\mu\nu\rho\lambda}\mathrm{tr}[\hat{V}_\mu]\mathrm{tr}[T\hat{V}_\nu]\mathrm{tr}[T[\hat{V}_\rho,\hat{V}_\lambda]] \\
& + ig'\alpha_{27}\epsilon^{\mu\nu\rho\lambda}\mathrm{tr}[\hat{V}_\mu]\mathrm{tr}[T\hat{V}_\nu]B_{\rho\lambda} + ig\alpha_{28}\epsilon^{\mu\nu\rho\lambda}\mathrm{tr}[\hat{V}_\mu]\mathrm{tr}[T\hat{V}_\nu]\mathrm{tr}[TW_{\rho\lambda}] \\
& + g\alpha_{29}\epsilon^{\mu\nu\rho\lambda}\mathrm{tr}[\hat{V}_\mu]\mathrm{tr}[\hat{V}_\nu W_{\rho\lambda}] + ig''\alpha_{30}\epsilon^{\mu\nu\rho\lambda}X_{\mu\nu}\mathrm{tr}[T[\hat{V}_\rho,\hat{V}_\lambda]] + ig''\alpha_{31}X_{\mu\nu}\mathrm{tr}[T[\hat{V}^\mu,\hat{V}^\nu]] \\
& + g''\alpha_{32}\epsilon^{\mu\nu\rho\lambda}\mathrm{tr}[\hat{V}_\mu]\mathrm{tr}[T\hat{V}_\nu]X_{\rho\lambda} + \alpha_{33}\mathrm{tr}[\hat{V}_\mu]\mathrm{tr}[T\hat{V}_\nu]\mathrm{tr}[T[\hat{V}^\mu,\hat{V}^\nu]] + g'g''\alpha_{34}\epsilon^{\mu\nu\rho\lambda}B_{\mu\nu}X_{\rho\lambda} \\
& + gg''\alpha_{35}\epsilon^{\mu\nu\rho\lambda}X_{\mu\nu}\mathrm{tr}[TW_{\rho\lambda}] + ig'\alpha_{36}\mathrm{tr}[\hat{V}_\mu]\mathrm{tr}[T\hat{V}_\nu]B^{\mu\nu} + ig\alpha_{37}\mathrm{tr}[\hat{V}_\mu]\mathrm{tr}[T\hat{V}_\nu]\mathrm{tr}[TW^{\mu\nu}] \\
& + g\alpha_{38}\mathrm{tr}[\hat{V}^\mu]\mathrm{tr}[\hat{V}^\nu W_{\mu\nu}] + g''\alpha_{39}\mathrm{tr}[\hat{V}_\mu]\mathrm{tr}[T\hat{V}_\nu]X^{\mu\nu} + ig\alpha_{40}\mathrm{tr}[\hat{V}^\mu]\mathrm{tr}[T\hat{V}^\nu W_{\mu\nu}]
\end{aligned} \tag{2.6}$$

among which $\alpha_1, \alpha_8, \alpha_{24}, \alpha_{25}$ are kinetic mixing parameters; $\alpha_{12} \sim \alpha_{14}$, α_{30}, $\alpha_{33} \sim \alpha_{40}$ are associated with CP-violation terms. The anomalous term $\mathcal{L}_A$ is

$$\mathcal{L}_A = \alpha_{42}g^2\epsilon^{\mu\nu\rho\lambda}tr[W_{\mu\nu}W_{\rho\lambda}] + \alpha_{43}g'^2\epsilon^{\mu\nu\rho\lambda}B_{\mu\nu}B_{\rho\lambda} + g''^2\alpha_{44}\epsilon^{\mu\nu\rho\lambda}X_{\mu\nu}X_{\rho\lambda} \tag{2.7}$$

With the exception of the kinetic term $\mathcal{L}_K$ in $\mathcal{L}_4$, the α_i $(i = 1, \cdots, 14)$ correspond to terms appearing in the conventional electroweak chiral Lagrangian (EWCL) [43] without Z', α_j $(j = 15, \cdots, 44)$ correspond to terms in the EEWCL involving Z'. In the rest of the

JHEP05(2014)088

paper, we shall ignore the CP-violation terms and the anomaly terms. This constitutes our third and fourth assumptions. Our fifth assumption is to forbid possible mixing between the Z' and the electroweak bosons γ, Z in order to keep the Z' dark. This implies that the gauge eigenstate X_μ can be identified with the physical state Z'_μ. No mass mixing requires $\beta_2 = 0$, and no kinetic mixing leads to $\alpha_{24} = \alpha_{25} = 0$. Furthermore, we need to set to zero the Stueckelberg coupling $\tilde{g}' = 0$. At this point it is important to stress that there are mixing parameters which do not involve the Z': β_1 is a mass mixing term among SM gauge bosons, thus it will induce a correction to the ρ parameter (T parameter), while α_1 and α_8 induce kinetic mixings, thus generating a contribution to the S parameter. The remaining β_3 generates a contribution to the mass of the Z', which is given by

$$M_{\mathrm{Z}'} = g'' f \sqrt{1 - 2\beta_3}. \tag{2.8}$$

With the above five assumptions, the p^4-order EEWCL (2.4) in the unitary gauge gives the following Lagrangian up to quartic couplings:

$$\begin{aligned}\mathcal{L} = & -\frac{1}{4}V_{\mu\nu}V^{\mu\nu} - \frac{1}{2}W^+_{\mu\nu}W^{-\mu\nu} + iC_{V-+}V_{\mu\nu}W^{+\mu}W^{-\nu} + iC_{+V-}(W^+_{\mu\nu}W^{-\mu}V^\nu - W^-_{\mu\nu}W^{+\mu}V^\nu) \\ & + iC_{V_1V_2V_3}V_1^{\mu\nu}V_{2\mu}V_{3\nu} + D_{++--}W^+_\mu W^{+\mu}W^-_\nu W^{-\nu} + D_{+-+-}W^+_\mu W^{-\mu}W^-_\nu W^{+\nu} \\ & + D_{+-V_1V_2}W^+_\mu W^{-\mu}V_{1\nu}V_2{}^\nu + D_{+V_1-V_2}W^+_\mu V_1^\mu W^-_\nu V_2^\nu + D_{V_1V_2V_3V_4}V_{1\mu}V_2^\mu V_{3\nu}V_4^\nu. \end{aligned} \tag{2.9}$$

Here V_i denotes the neutral gauge bosons Z, γ, and Z', and the various C and D coefficients in terms of the α_i and β_i coefficients are given in appendix A. Note that, with our fifth assumption of no mass mixing, $C_{V_1V_2V_3}$ vanishes.

In order to keep the Z' stable, we need to impose the vanishing of vertices that are linear in the Z' field; this constitutes our sixth assumption. For the triple couplings $C_{Z'-+}$ and $C_{+Z'-}$ to vanish, we need to set $\alpha_{31} = 0$; there is then no triple coupling involving Z' (note that without the triple coupling $C_{Z'VV}$ with $V = \gamma, Z, W^\pm$, the longitudinal W and Z scattering will not involve Z' at tree level and that imposes no unitarity constraint on the Z' couplings). Left with four Z'-independent triple couplings, one $C_{+\gamma-}$ has fixed coefficients, which only depend on SM couplings, whereas the other three $C_{\gamma-+}, C_{Z-+}$, and C_{+Z-} are free, corresponding to independent coefficients α_2, α_3, and α_9. For quartic couplings, $D_{+-ZZ'} = 0$ leads to $\alpha_{16} = 0$, $D_{+Z-Z'} = D_{+Z'-Z} = 0$ leads to $\alpha_{17} = 0$, and $D_{Z'ZZZ} = -g_Z^3 g''(2\alpha_{15}+\alpha_{16}+\alpha_{17}) = 0$ further leads to $\alpha_{15} = 0$. (Note that if the Stueckelberg coupling $\tilde{g}'$ does not vanish, it will also generate nonzero $D_{+-ZZ'}$, $D_{+Z-Z'}$, $D_{+-AZ'}$, $D_{+A-Z'}$.) We are finally left with 16 nonzero quartic couplings. Among them, $D_{+-\gamma\gamma}$ and $D_{+\gamma-\gamma}$ also have fixed coefficients and are not free. The other four $D_{+-\gamma Z}$, $D_{+\gamma-Z}$ and $D_{+Z-\gamma} = D_{+\gamma-Z}$ only rely on α_3 and then are related to the triple vertex. The remaining 11 nonzero quartic couplings $D_{++--}, D_{+-+-}, D_{+-ZZ}, D_{+-Z'Z'}, D_{+Z-Z}, D_{+Z'-Z'}$, $D_{ZZZZ}, D_{Z'Z'ZZ}, D_{Z'ZZ'Z}, D_{Z'Z'Z'Z}, D_{Z'Z'Z'Z'}$ are free, corresponding to the 11 independent coefficients α_4 to α_7, α_{10}, and α_{18} to α_{23}. In table I, we list details of all the triple and quartic couplings.

Given the six assumptions stated above:

(i) no direct coupling to the Higgs;

(ii) no direct coupling to fermions;

JHEP05(2014)088

couplings	exist in SM (modified by)	independent	control by	vanishing condition
$C_{\gamma-+}$	yes ($\alpha_{2,3,9}$)	-	-	-
C_{Z-+}	yes ($\alpha_{2,3,9}$)	-	-	-
$C_{Z'-+}$	no	yes	α_{31} & $\tilde{g}'$	$\alpha_{31} = \tilde{g}' = 0$
$C_{+\gamma-}$	yes (not modified)	-	-	-
C_{+Z-}	yes (α_3)	-	-	-
$C_{+Z'-}$	no	-	$\tilde{g}'$	$\tilde{g}' = 0$
$C_{V_1V_2V_3}$	no	-	-	always
D_{++--}	yes ($\alpha_{3,4,9}$)	-	-	-
D_{+-+-}	yes ($\alpha_{3,4,5,9}$)	-	-	-
$D_{+-\gamma\gamma}$	yes (not modified)	-	-	-
D_{+-ZZ}	yes ($\alpha_{3,5,7}$)	-	-	-
$D_{+-Z'Z'}$	no	yes	α_{21}	-
$D_{+-\gamma Z}$	yes (α_3)	-	-	-
$D_{+-\gamma Z'}$	no	-	$\tilde{g}'$	$\tilde{g}' = 0$
$D_{+-ZZ'}$	no	yes	α_{16} & $\tilde{g}'$	$\alpha_{16} = \tilde{g}' = 0$
$D_{+\gamma-\gamma}$	yes (not modified)	-	-	-
D_{+Z-Z}	yes ($\alpha_{3,4,6}$)	-	-	-
$D_{+Z'-Z'}$	no	yes	α_{19}	-
$D_{+\gamma-Z}$	yes (α_3)	-	-	-
$D_{+\gamma-Z'} = D_{+Z'-\gamma}$	no	-	$\tilde{g}'$	$\tilde{g}' = 0$
$D_{+Z-\gamma} = D_{+\gamma-Z}$	yes	-	-	-
$D_{+Z-Z'} = D_{+Z'-Z}$	no	yes	α_{17} & $\tilde{g}'$	$\alpha_{17} = \tilde{g}' = 0$
D_{ZZZZ}	no	yes	α_{10}	-
$D_{Z'ZZZ}$	no	yes	α_{15}	$2\alpha_{15}+\alpha_{16}+\alpha_{17}=0$
$D_{Z'Z'ZZ}$	no	yes	α_{20}	-
$D_{Z'ZZ'Z}$	no	yes	α_{18}	-
$D_{Z'Z'Z'Z}$	no	yes	α_{22}	$\alpha_{22} = 0$
$D_{Z'Z'Z'Z'}$	no	yes	α_{23}	-

Table 1. List of triple and quartic couplings.

(iii) no CP violating terms in the EEWCL;

(iv) no anomalous terms in the EEWCL;

(v) no kinetic nor mass mixing terms;

(vi) no single Z' couplings;

we are finally left with four Z'-dependent quartic vertices each involving two Z' fields,

$$D_{+-Z'Z'} \equiv g_1 = 4g^2 g''^2(\alpha_5 + \alpha_{21}) \tag{2.10}$$

JHEP05(2014)088

$$D_{+Z'-Z'} \equiv g_2 = 4g^2 g''^2(\alpha_4 + \alpha_{19}) \tag{2.11}$$

$$D_{Z'Z'ZZ} \equiv g_3 = g_Z^2 g''^2(\alpha_5 + 2\alpha_7 + 4\alpha_{20} + 2\alpha_{21}) \tag{2.12}$$

$$D_{Z'ZZ'Z} \equiv g_4 = 4g_Z^2 g''^2(\alpha_4 + \alpha_6 + 2\alpha_{18} + \alpha_{19}) \tag{2.13}$$

where $g_Z^2 = g^2 + g'^2$. Here we limit ourselves to vertices with up to 4 particles: the EEWCL does contain Z' vertices with more gauge boson, however their physical effect is subleading and we will not consider them any further. The above couplings do contribute to electroweak precision tests at loop level: such contributions are log-divergent, and their contribution can be absorbed in the tree-level contributions β_1 and $\alpha_{1,8}$, whose values are therefore strongly constrained. In the following we will therefore not consider bounds from precision tests, as they do not give unique indication on the size of the quartic couplings listed above. Up to now, we have not successfully built the detail underlying model which satisfy above six constraints and have nonzero four point vertices of (10)-(13), we leave this model construction to future investigations. To keep the number of free parameters to a minimum, we shall take in our analysis a unique coupling constant g_0 and consider five different arrangements of coupling constants as follows:

- universal case: $g_1 = g_2 = 4g^2 g_0$, $g_3 = \frac{3}{8} g_4 = \frac{3}{2} g_Z^2 g_0$, or $\alpha_4 = \alpha_5 = \alpha_{19} = \alpha_{21} \equiv \frac{g_0}{2g''^2}$, $\alpha_6 = \alpha_7 = \alpha_{18} = \alpha_{19} = \alpha_{20} = 0$
- case 1: $g_1 = 4g^2 g_0$, $g_3 = \frac{3}{2} g_Z^2 g_0$, $g_2 = g_4 = 0$, or $\alpha_5 = \alpha_{21} \equiv \frac{g_0}{2g''^2}$, $\alpha_4 = \alpha_6 = \alpha_7 = \alpha_{18} = \alpha_{19} = \alpha_{20} = 0$
- case 2: $g_2 = 4g^2 g_0$, $g_4 = 4g_Z^2 g_0$, $g_1 = g_3 = 0$, or $\alpha_4 = \alpha_{19} \equiv \frac{g_0}{2g''^2}$, $\alpha_5 = \alpha_6 = \alpha_7 = \alpha_{18} = \alpha_{20} = \alpha_{21} = 0$
- case 3: $g_3 = 3g_Z^2 g_0$, $g_1 = g_2 = g_4 = 0$, or $\alpha_7 = \alpha_{20} \equiv \frac{g_0}{2g''^2}$, $\alpha_4 = \alpha_5 = \alpha_6 = \alpha_{18} = \alpha_{19} = \alpha_{21} = 0$
- case 4: $g_4 = 6g_Z^2 g_0$, $g_1 = g_2 = g_3 = 0$, or $\alpha_6 = \alpha_{18} \equiv \frac{g_0}{2g''^2}$, $\alpha_4 = \alpha_5 = \alpha_7 = \alpha_{19} = \alpha_{20} = \alpha_{21} = 0$.

The strategy of taking these choices is that: first, we try to keep the SM factors explicit and then the bounds are shown on $g''^2\alpha_i$ (where g'' is related to the mass of the Z', thus a physical connection). Second, for universal case, we try to balance all of four vertices couplings by requiring $g_1 = g_2$ and $g_3 = 3g_4/8$. Third, for remaining four cases, we focus on α_i coefficients appeared in the original EEWCL. Considering that there are eight couplings $\alpha_4, \alpha_5, \alpha_6, \alpha_7, \alpha_{18}, \alpha_{19}, \alpha_{20}, \alpha_{21}$ enter into effective four point vertices, we take the corresponding four couplings g_1, g_2, g_3, g_4 are generated by specific operator pairs, so it would make sense to follow the patterns suggested by each type of operator pairs, as follows: α_5, α_{21} generate case 1; α_4, α_{19} generate case 2; α_7, α_{20} generate case 3; α_6, α_{18} generate case 4.

In the following sections, we shall mainly focus on the above five cases and derive information on the unique coupling g_0 when discussing possible constraints from various experiments. Some possible exceptions are also discussed.

JHEP05(2014)088

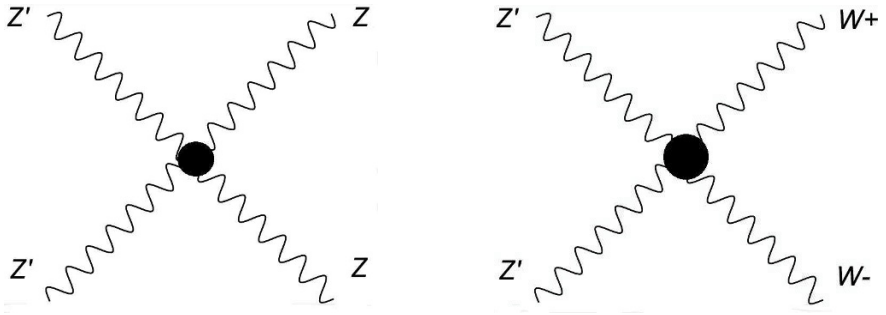

Figure 1. Two annihilation processes of Z' to SM weak gauge bosons.

3 Relic density constraint of dark Z'

In the standard Cosmology picture (ΛCDM), it is assumed that the DM particles are in thermal equilibrium with the other SM particles via various fundamental processes such as $Z'Z' \to \bar{P}P$ where P is any SM particle. In the high-temperature Early Universe, DM particles were kept in thermal equilibrium as long as the reaction rate, scaled by the temperature, was faster than the expansion rate H (the Hubble parameter) of the Universe. The Universe cooled down as it continued to expand. At temperatures around which the reaction rate fell below the expansion rate H, the DM particles began to decouple from the thermal bath. The DM particles will continue to annihilate into SM particles up until the point when they no longer encounter one another. The remaining DM particles will then become the relics that we can observe today. The two possible annihilation processes for our dark Z' are shown in figure 1. Their annihilation rates to SM weak gauge bosons are

$$\sigma_W\, v = \frac{\sqrt{1-\frac{1}{r_W^2}}}{9\times 64\pi m_{Z'}}\Big\{[(224r_W^4+112r_W^2+136)g_1^2-(160r_W^4+80r_W^2+176)g_1g_2+(152r_W^4+128r_W^2+96)g_2^2] + \Big[(88r_W^4-40r_W^2+56)g_1^2-\Big(\frac{304}{3}r_W^4+32r_W^2+\frac{32}{3}\Big)g_1g_2+\Big(24r_W^4+\frac{112}{3}r_W^2-\frac{4}{3}\Big)g_2^2\Big]v^2\Big\} \quad (3.1)$$

$$\sigma_Z\, v = \frac{\sqrt{1-\frac{1}{r_Z^2}}}{18\times 64\pi m_{Z'}}\Big\{[(224r_Z^4+112r_Z^2+136)g_3^2-(160r_Z^4+80r_Z^2+176)g_3g_4+(152r_Z^4+128r_Z^2+96)g_4^2] + \Big[(88r_Z^4-40r_Z^2+56)g_3^2-\Big(\frac{304}{3}r_Z^4+32r_Z^2+\frac{32}{3}g_3g_4+\Big(24r_Z^4+\frac{112}{3}r_Z^2-\frac{4}{3}\Big)g_4^2\Big]v^2\Big\}, \quad (3.2)$$

in which $r_W = m_{Z'}/m_W$ and $r_Z = m_{Z'}/m_Z$, and v is the relative velocity of the colliding DM particles. In above result, due to the non-relativistic characteristics of our dark Z', we have taken expansion in terms of powers of v up to the order of v^2. Note that for these annihilations to arise, the mass of Z' should be heavier than the mass of the SM weak gauge bosons. If the Z' mass is lighter than the SM weak boson mass, we instead use the loop-induced effective $Z'Z'q\bar{q}$ vertices given in the next section. The corresponding annihilation rate is

$$\sigma\, v = \frac{v^2}{6}\Big[\frac{1}{6\pi}\sum_f\Big(\frac{K_{V,f}}{\sqrt{2}}\Big)^2 c_f\sqrt{1-\frac{m_f^2}{M_{Z'}^2}}M_{Z'}^2\Big(2+\frac{m_f^2}{M_{Z'}^2}\Big)+\frac{1}{3\pi}\sum_f\Big(\frac{K_{VA,f}}{\sqrt{2}}\Big)^2 c_f\Big(1-\frac{m_f^2}{M_{Z'}^2}\Big)^{3/2}M_{Z'}^2\Big], \quad (3.3)$$

where $K_{V,f}$ and $K_{VA,f}$ are the effective couplings introduced in the next section in eq. (4.1), and c_f is the color index, which is 1 for leptons and 3 for quarks.

JHEP05(2014)088

The relic density is calculated by solving the Boltzmann equation in the standard approximation procedure [44],

$$\Omega_{\rm WIMP}h^2 = \frac{1.07\times10^9}{m_{pl}}\frac{x_F GeV^{-1}}{\sqrt{g_{*S}}}\frac{1}{a+3b/x_F}, \tag{3.4}$$

where h is the scaled Hubble constant, $x_F = m_{Z'}/T_F$ with T_F the freezing temperature, $m_{pl} = 1.22\times10^{19}GeV$, g_{*S} the total number of effectively relativistic degrees of freedom at freeze-out temperature, and a and b are parameters in the expansion $\sigma v = a+bv^2+\mathcal{O}(v^4)$. The freeze-out temperature parameter x_F can be evaluated by numerically solving the following equation:

$$x_F = \ln\left[c(c+2)\sqrt{\frac{45}{8}}\frac{g m_{Z'} m_{pl}(a+6b/x_F)}{2\pi^3\sqrt{g_{*S}}x_F^{1/2}}\right], \tag{3.5}$$

where $g = 3$ is the number of degrees of freedom for the Z' DM, and c is a numerical constant usually taken equal to 1/2. With DM mass ranging from GeV to TeV, $x_F \approx 25$ and remains essentially constant. In our numerical analysis, we demand that the resulting relic density be less than the measured value from PLANCK $\Omega_{\rm WIMP}h^2 = 0.1199\pm0.0027$ at 68%CL [45], which leads to constraints for the effective coupling constants $g_i,\ i = 1,2,3,4$ and the dark Z' mass $M_{Z'}$. The result of the five different coupling arrangements introduced at the end of section II for $M'_Z > 100$GeV is shown in figure 2, where we have used result (3.1) and (3.2) to perform our calculation. Note that because the ordinate is logarithmically scaled, the diagram would be unable to show clearly the possible deviations of several percent from the experiment, and hence are not plotted. For dark Z' masses below the W mass threshold, we instead use eq. (3.3) to perform our estimation; the results are shown in figure 3. Note that in the intermediate region $m_W/2 < M_{Z'} < m_W$, the three-body process $Z'Z' \to WW^*(ZZ^*)$, where one of the two gauge bosons is off-shell, is also relevant: we expect it to smoothly interpolate between the results in figure 2 and 3. Nevertheless, below the WW threshold, the coupling is required to be very large, and this region is excluded by direct-detection experiments, as we will show in the next section.

4 Effective quark vertex and direct detection of dark Z'

In this section, we discuss the direct-detection constraints on dark Z'. Direct-detection experiments are designed to measure the recoil energy of the atomic nuclei following DM elastic scattering. DM-quark interactions will naturally induce DM-nucleon interactions, and the latter further induce DM-nucleus interactions. Such interactions may be detected in underground direct-detection experiments.

As our second assumption does not allow Z' to directly couple to SM fermions (fermiophobic), it can only couple indirectly to quarks through the SM gauge-boson loop depicted in figure 4. This loop diagram leads to finite effective vector-vector and vector-axial-vector interaction vertices [42]:

$$\mathcal{L}_{\rm eff} = \Sigma_q\frac{K_{V,q}}{\sqrt{2}}(Z'^*_\nu i\overleftrightarrow{\partial}_\mu Z'^\nu)\bar{q}\gamma^\mu q + \Sigma_q\frac{K_{VA,q}}{\sqrt{2}}(Z'^*_\nu i\overleftrightarrow{\partial}_\mu Z'^\nu)\bar{q}\gamma^\mu\gamma_5 q. \tag{4.1}$$

JHEP05(2014)088

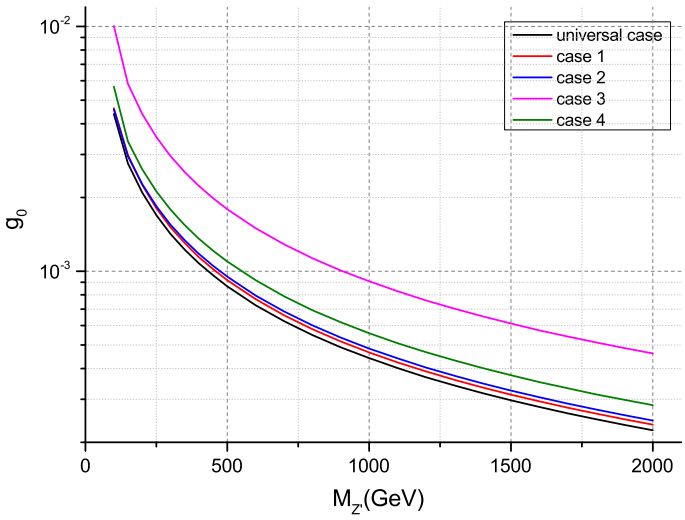

Figure 2. Predicted unique coupling constant g_0 as a function of DM mass $m_{Z'} \geq 100$GeV fixed by the observed relic density. Each color of the curves represents different arrangements of coupling constant g_i. The allowed region is located above the curve.

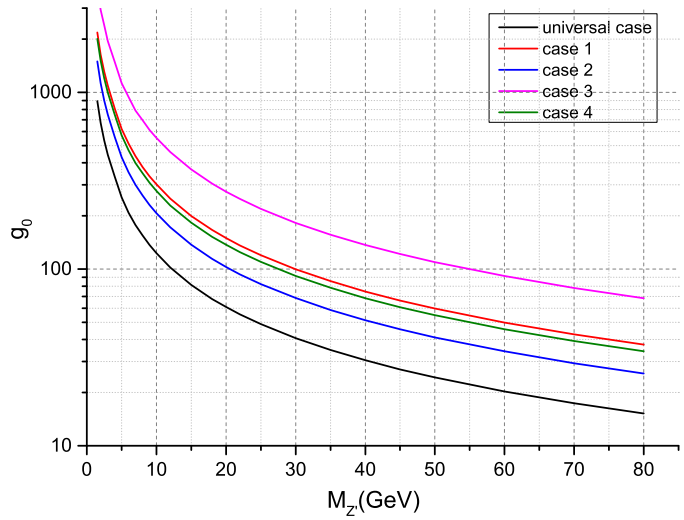

Figure 3. Same as for figure 1 but with DM mass $m_{Z'} \leq 80\,\text{GeV}$.

The finiteness of this loop-induced $Z'Z'\bar{q}q$ vertex implies that our fermiophobic assumption is consistent by itself. Furthermore, the structure of the above result for the effective vertices only generates spin-independent (SI) interaction. Hence there will be no constraint from the cross-section of the spin-dependent interaction.

JHEP05(2014)088

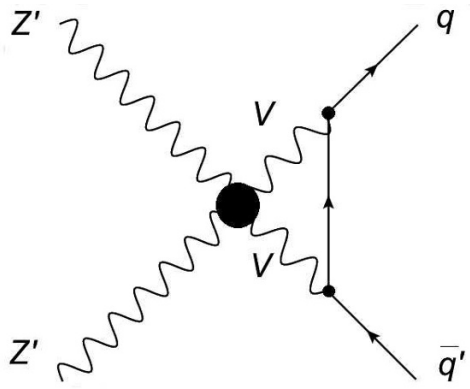

Figure 4. Dark matter scattering from quarks through SM gauge-boson loops.

Note that the velocity of DM near the Earth is considered to be $v \approx 0.001c$; for low-energy SI interactions, only the vector interaction survives. The cross-section is then given by

$$\sigma_{V,Z'N} = \frac{m_N^2 m_{Z'}^2}{\pi(m_{Z'} + m_N)^2}\left(\frac{K_{V,N}}{\sqrt{2}}\right)^2, \tag{4.2}$$

where

$$K_{V,p} = 2K_{V,u} + K_{V,d}, \quad K_{V,n} = K_{V,u} + 2K_{V,d} \tag{4.3}$$

$$\frac{K_{V,q}}{\sqrt{2}} = \frac{(g_1+g_2)(c_q^2+c_q'^2)}{32\pi^2 m_W^2} + \frac{(g_3+g_4)(c_q^2+c_q'^2)}{32\pi^2 m_Z^2} \tag{4.4}$$

and c_q and c_q' for $q = u, d$ are coefficients associated with SM couplings

$$c_u = \frac{ig}{4\cos\theta_W}\left(1 - \frac{8}{3}\sin^2\theta_W\right), \qquad c_d = \frac{ig}{4\cos\theta_W}\left(-1 + \frac{4}{3}\sin^2\theta_W\right),$$
$$c_u' = \frac{ig}{4\cos\theta_W}, \qquad c_d' = -\frac{ig}{4\cos\theta_W}. \tag{4.5}$$

The curves for the predicted cross-section σ vs $m_{Z'}$ with different coefficient settings are shown in figure 5. The upper bounds set by the XENON100 2012 data [46], the latest LUX result [47] and SuperCDMS result [48] are also plotted in figure 5.

We next discuss some of these results:

- Because the unique coupling g_0 is constrained to order 10^{-2} in the typical few tens to few hundreds GeV region (see figure 5), it is natural to ask if we go beyond the limitations set for the five arrangements and consider arbitrary g_i couplings; is there a possibility to enhance the value of the coupling? To examine this issue, note that eq. (4.4) gives $K_{V,q}$, which then determines the final cross-section σ; it depends on $g_1 + g_2$ and $g_3 + g_4$. If we take $g_1 \approx -g_2 = 4g^2 g_0$, $g_3 \approx -g_4 = 4g_Z^2 g_0$, then we achieve an arbitrary small $K_{V,q}$ and subsequently an arbitrary small scattering cross-section. For example, $g_2 = -0.9g_1$, $g_4 = -0.9g_3$, and $g_1 = g_3$ leads to $K_{V,q} \propto 0.1g_1$, which is already smaller by an order of magnitude than the five cases already derived in

JHEP05(2014)088

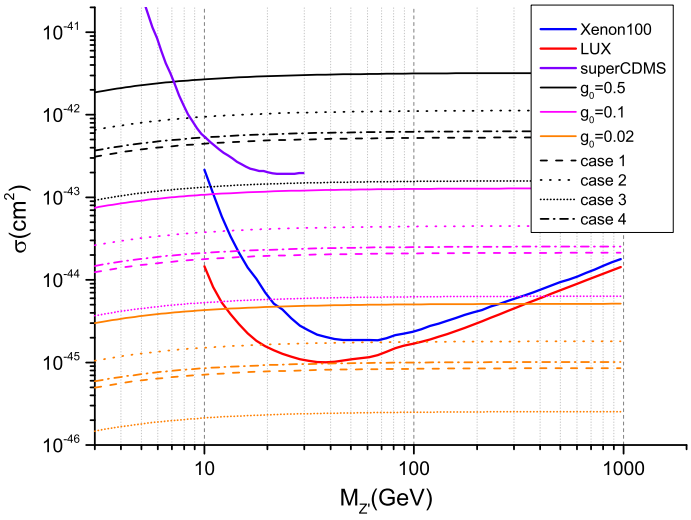

Figure 5. Predicted spin-independent WIMP-proton cross-sections for dark Z'. The solid line is for the universal case, dashed line for case 1, dotted line for case 2, short dotted line for case 3, and dash-dotted line for case 4. For each case, the black lines correspond to $g_0 = 0.5$, magenta lines to $g_0 = 0.1$, and orange lines to $g_0 = 0.02$. Also, the upper bounds set by XENON100, LUX and SuperCDMS are marked in blue, red and purple respectively.

figure 5. Hence $\sigma \propto 0.01 g_1$ is less than those used in figure 5 by two orders of magnitudes and is equivalent to enhancing the constraint for g_0 by two order of magnitudes; i.e., it relaxes the constraint for g_0 from 10^{-2} to 10^0, because experimentally we must fix the cross-section. Therefore, we do have flexibility in the couplings in relaxing the constraints on g_0 (or α_i) from direct detection. In the next section, we shall see for indirect detection that this scenario does not arise as there exists no such coupling space.

- As we have introduced in our theory the one-loop-induced $Z'Z'\bar{q}q$ vertex (4.1), one may inquire of the role of the one-loop-induced $Z'Z'h$ vertex depicted in figure 6. One can easily check that this loop diagram is logarithmically divergent. This implies that our first higgsphobic assumption, introduced in sectionII, by which we ignore the direct coupling between Z' and Higgs is not consistence by itself. To cancel such a divergence, we have to introduce into the theory the tree-level vertex, $Z'Z'h$, which violates our higgsphobic assumption. Furthermore, once we have such a $Z'Z'h$ vertex, no matter whether it is a tree-level one added to the theory by hand or a loop-induced one, it can further decay via the Higgs-mediated s-channel (figure 7) into a fermion pair, which then leads to further corrections to the effective $Z'Z'\bar{q}q$ vertex given by eq. (4.1). The reason that we do not consider this correction is as follows: suppose we abandon our first assumption by introducing the tree-level $Z'Z'h$ vertex into our theory. The $Z'Z'h$ vertex then includes two contributions: one is a tree-level term, and the other a loop term (figure 6). After renormalisation, i.e., cancelling the loop-

JHEP05(2014)088

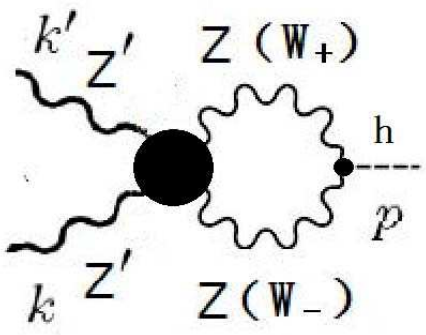

Figure 6. Dark matter annihilating into Higgs through SM gauge boson loops.

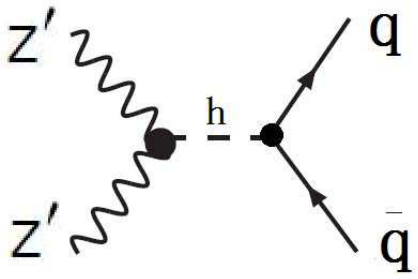

Figure 7. Dark matter annihilating to form a quark pair through the effective $Z'Z'h$ vertex.

induced divergence (figure 6) by the tree-level term, the remaining finite part should not be very much different with respect to the finite part of figure 6. This finite part of the $Z'Z'h$ vertex via the Higgs-mediated s-channel (figure 7) further leads to an effective $Z'Z'\bar{q}q$ vertex, which is of scalar type $Z'^2\bar{q}q$ or pseudo-scalar type $Z'^2\bar{q}\gamma_5 q$. These vertices have different vertex structures in comparison with the vector and axial vector vertices given by eq. (4.1). Only the scalar vertex survives and it contributes to the nucleon cross-section similar to that in (4.2), but has an extra factor proportional to $m_q^2/m_{Z'}^2 \sim 10^{-8}$ with m_q the mass of the u or d quark. This factor results from the replacement of the derivative-type vector coupling of (4.2) with the non-derivative-type scalar coupling $Z'Z'\bar{q}q$ (see ref. [42]). It is this suppression factor that allows us to ignore the loop-induced and tree-level $Z'Z'h$ vertices. Although our higgsphobic assumption is not consistent by itself, ignoring it only creates a very minor correction and thus we can still approximately adhere to it.

5 Indirect detection of dark Z'

In addition to the direct DM searches at underground laboratories, indirect searches look for DM annihilations or decay products in the atmosphere. These particles, which include neutrinos, gamma rays, positrons, and antiprotons, can be detected in cosmic-ray experiments. In this section, we discuss three of the latest experiments.

JHEP05(2014)088

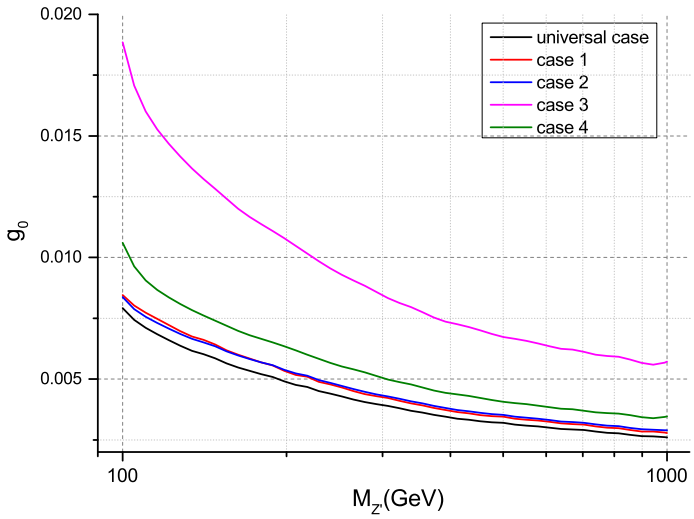

Figure 8. Upper bounds on the coupling constant g_0 from the PAMELA $\bar{p}/p$ flux ratio.

5.1 PAMELA experiment

We first follow the procedure in [42] to obtain constraints for Z' using the anti-proton to proton flux ratio $\bar{p}/p$ measured by the satellite-borne experiment PAMELA [49]. The tree-level annihilations $Z'Z' \to ZZ, WW$ contribute to the generation of the $\bar{p}/p$ signal via the hadronic decays of the W and Z bosons [50]. Together with the antiproton-to-proton flux ratio data of PAMELA, we can derive constraints for each of our five cases. The result is shown in figure 8, where the allowed region is below each curve. It should be noted that the loop-induced vertex Z'Z'qq given by eq. (4.1) can also contribute to the generation of the $\bar{p}/p$ signal. Nevertheless, our computations show that the constraint is very weak and we shall not discuss it here.

5.2 AMSII experiment

Recently, the AMSII collaboration has announced a new measurement of the cosmic-ray positron fraction [51]. We discuss DM annihilation in view of these measurements and derive constraints on our dark Z' matter mass and the universal case for coupling constant g_0. We consider the annihilation channels $Z'Z' \longrightarrow W^+W^-$ and $Z'Z' \longrightarrow ZZ$ as in the discussion for the relic density in the previous section, and use the same method in [52] to set conservative limits by requiring that the predicted positron flux remains smaller than the measured flux over all energies. For simplicity, we assume a standard Navarro-Frenk-White (NFW) density profile [53], i.e., $\bar{J}\Delta\Omega \approx 1$. The result is graphed in figure 9, which shown that it is not competitive with the PAMELA bounds.

JHEP05(2014)088

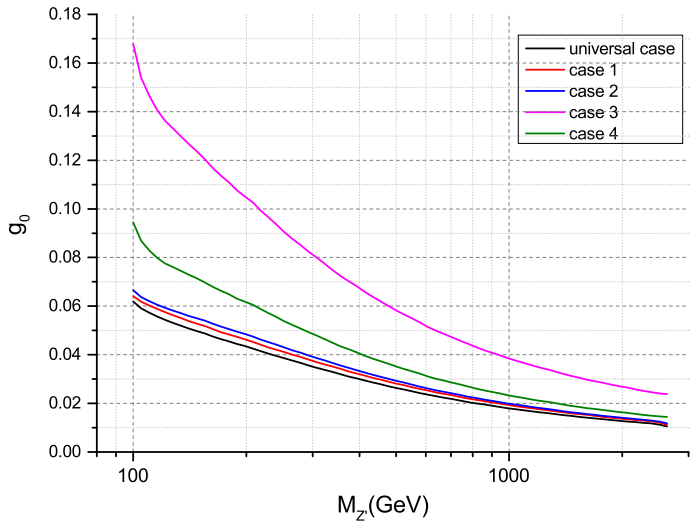

Figure 9. Upper bounds from AMSII cosmic-ray positron fraction spectrum.

5.3 FermiLAT experiment

Photons from DM annihilations in the centre of the galaxy provide another source of an indirect signal. As dark Z' cannot annihilate into photon pairs directly (we have checked that even by including one-loop corrections, the $Z'Z'\gamma$ vertex still vanishes), we can only detect continuum photon signals. The differential flux of the γ-rays observed on Earth from DM annihilation is as follows,

$$\frac{d\Phi}{dE_\gamma} = (5.5 \times 10^{-10} s^{-1} cm^{-2}) \frac{dN}{dE_\gamma} \left(\frac{\langle \sigma v \rangle}{pb}\right) \left(\frac{100GeV}{m_\chi}\right)^2 \bar{J} \Delta\Omega. \tag{5.1}$$

Again, as in the previous subsection, we have assumed the DM distribution to follow the NFW profile. The annihilation cross-section is

$$\langle \sigma v \rangle \approx a + b\langle v^2 \rangle = a + 2b\bar{v}^2, \tag{5.2}$$

where $\bar{v} = 270 km/s$. The simple analytic fit is as follows [54]

$$\frac{dN}{dE_\gamma} = \frac{dN}{m_\chi dx} = \frac{1}{m_\chi} \frac{a_0}{x^{1.5}} e^{-b_0 x}, \tag{5.3}$$

where $x = E_\gamma/m_\chi$, $a_0 = 0.73$, and $b_0 = 7.76$ for W/Z bosons. We consider the universal case with g_0 fixed by the relic density for different DM masses; the predicted γ-ray spectra is shown in figure 10. From it we can see the photon energy flux is about 3 orders of magnitude lower than the experiment data. To explain the discrepancy with the data, we will need an enhancement of 300 to 8000. The required boost factors are obtained by fitting the data and the result is shown in figure 11.

JHEP05(2014)088

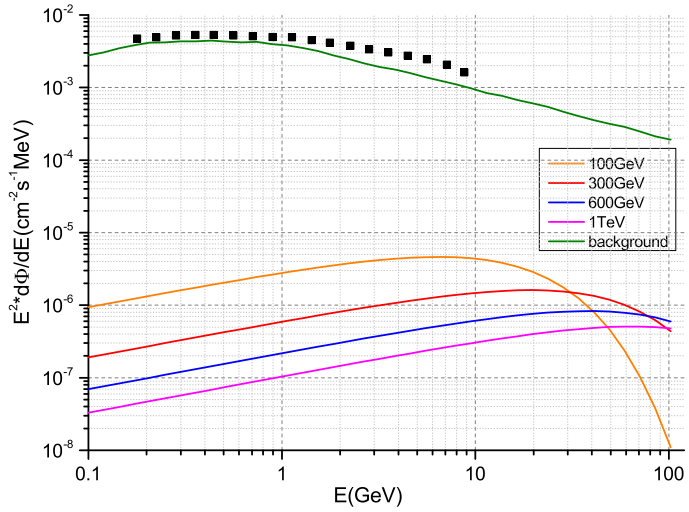

Figure 10. Predicted γ-ray spectra for the annihilation of dark Z' in the universal case and with a NFW density profile. The FermiLAT observation data are also presented.

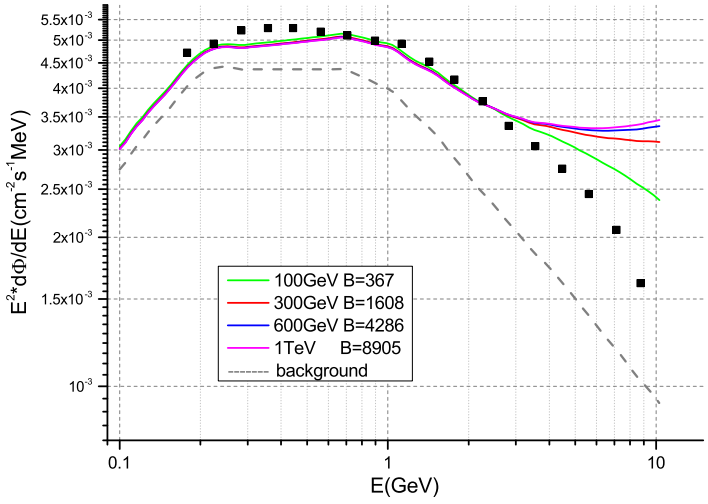

Figure 11. Comparison of predicted dark Z' signals for different masses and boost factors with FermiLAT observation data.

Recently, γ-ray observations of 25 Milky-Way dwarf spheroidal satellite galaxies from four years of FermiLat data was reported in [55]. We can use the constraint for the channel $Z'Z' \to W^+W^-$ in [55] to give upper limits to coefficients g_1 and g_2. The result is shown below in figure 12.

With the above discussion of the five g_0 cases, we may ask a similar question to that of the last section: if we go beyond the five limit cases discussed above and consider arbitrary

JHEP05(2014)088

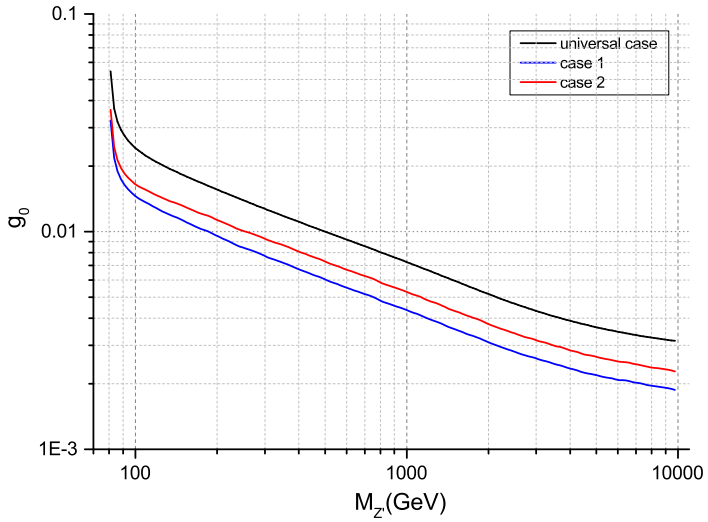

Figure 12. Upper limits to the dark-Z' coupling constant g_0 for the universal case, case 1, and case 2 from FermiLAT γ-ray data.

g_i couplings, is there a possibility to enhance the value of the couplings? To answer this question, note that the contributions to cross-section for indirect detection are given by eq. (3.1) and eq. (3.2), in which the terms proportional to v^2 play very little role as v^2 is small. We can demand that the remaining terms take minimum values (which result in the smallest indirect-detection cross-section) to fix the coupling. For $m_{Z'} = 100\,GeV$ (the result changes little in the range 100 GeV$< m_{Z'} <$1 TeV), we find two minima:

$$g_2 \approx 0.521 g_1, \quad g_3 = g_4 = 0 \qquad \text{or} \qquad g_1 = g_2 = 0, \quad g_4 \approx 0.5207 g_3. \tag{5.4}$$

This result gives the same sign for g_1 and g_2, and for g_3 and g_4. This differs from the result in the direct detection discussed in the last section, where we obtain opposite signs for g_1 and g_2 and for g_3 and g_4. Further, in plotting the constraint for these two extreme cases (figure 13), we find that the PAMELA experiment still yields constraint $g_0 < 3 \times 10^{-2}$. This shows that, all in all, the constraint on the coupling is rather robust.

6 Combined result and other DM related issues

As the Z' is the only DM particle in our theory, we can discuss its mass $M_{Z'}$ and unique coupling g_0 in a $g_0 - M_{Z'}$ plot. For simplicity, we only discuss the universal case. Combining all effective phenomenological constraints from the last three sections, we obtain figure 14, where the shaded region is excluded by the different experiments. The allowed region has a the left boundary at roughly $M_{Z'} \sim 100$ GeV: below this mass scale, the relic density constraint from figure 3 already contradicts data from the XENON100 and LUX experiments. The lower bound above $M_{Z'} = 100$ GeV is the red curve from the relic density (figure 2), while the upper bound is from the PAMELA $\bar{p}/p$ flux ratio constraint (figure 8).

JHEP05(2014)088

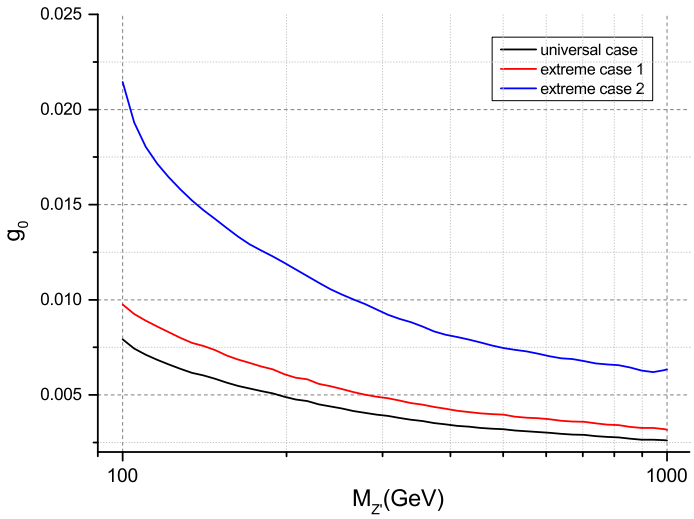

Figure 13. Upper bounds from the PAMELA experiment on the coupling constant g_0 for dark Z' in two extreme cases compared with the universal case.

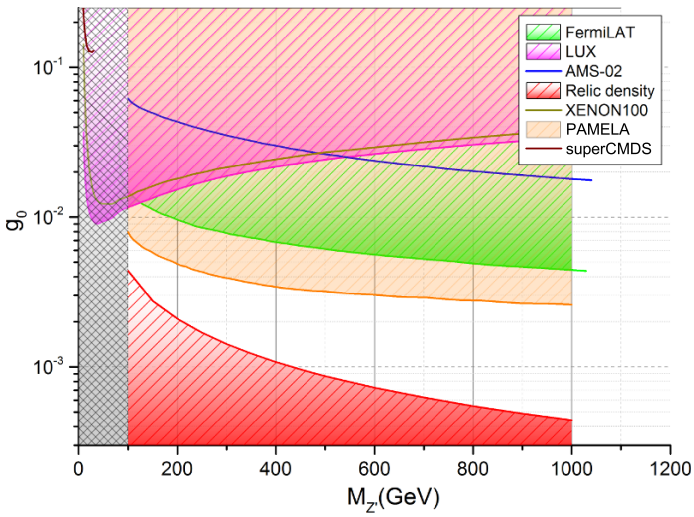

Figure 14. Combined constraints on coupling constants g_0 of dark Z' for the universal case.

We find g_0 is restricted to the region of $10^{-3} \sim 10^{-2}$. As discussed in the previous sections, this bound is quite solid, and it does depend mildly on the configuration of couplings.

Considering the low-energy region below the threshold of the W boson mass, the relic density from figure 3 offers a very strong constraint, which combined with the direct-detection results kills any possibility of the existence of a dark Z' in this low mass re-

JHEP05(2014)088

gion. If we simply ignore this fact, then a small dark Z' mass is allowed in this lower energy region. Currently, though, tensions exist among the different direct-detection experiments in the low-energy region. For example, null results from CDMS Ge, XENON, LUX and SuperCDMS challenge the CoGeNT/DAMA and latest CDMS SI results. Because different experiments use different detection materials with different numbers of proton/neutrons, isospin-violating DM may weaken these tensions. It was demonstrated that isospin-violating DM with $f_p/f_n \approx$-0.7 may alleviate the problem [56]. For our dark Z', f_q is given as follows:

$$\frac{f_q}{\sqrt{2}} = \frac{(g_1+g_2)(c_q^2+c_q'^2)}{32\pi^2 m_W^2} + \frac{(g_3+g_4)(c_q^2+c_q'^2)}{32\pi^2 m_Z^2} \tag{6.1}$$

$$f_p = 2f_u + f_d, \qquad f_n = f_u + 2f_d. \tag{6.2}$$

One can check that

$$\frac{f_u}{f_d} = \frac{c_u^2 + c_{u'}^2}{c_d^2 + c_{d'}^2}, \tag{6.3}$$

which further leads to

$$f_p/f_n \approx 0.93. \tag{6.4}$$

Clearly, the ratio is completely unrelated to the coupling constants g_1, g_2, g_3, and g_4. Our dark Z' itself cannot give $f_p/f_n < 0$ (adding in Higgs boson may bring new vertices and change the rate). Indeed, it was recently observed that the LUX [47] and SuperCDMS [48] data are in strong contrast [57–59] with the CDMS-Si signal result [60], even for isospin-violating DM (IVDM) where the ratio of the proton-to-neutron couplings can be maximally "xenophobic". Another possibility to reconcile this tension is to consider an inelastically scattering DM model or an exothermic DM model [61]. However, to realise inelastic scattering, we need at least two DM states. As our simplest dark Z' model only has one state, the present dark Z' cannot produce inelastic scattering. This statement can be weakened in models where the Z' belongs to a triplet, i.e. it is accompanied by a W': this can be achieved in a chiral lagrangian with an extra SU(2) symmetry [62]. Remaining in our framework, we obtain the result that even if we ignore the strong constraint allowing our dark Z' to survive into the low-energy region, it still cannot reduce the tension among those observed possible DM signals with other null result experiments.

Finally, we need to discuss the impact of our dark Z' model on other experiments in particle physics. First, following our second and sixth assumptions, there are no mixing of the Z' with the Z and photon and no linear couplings of the Z'. This implies that there are no tree level bounds on the Z' couplings and mass from electroweak precision measurements [63]. However, loops of the $Z'Z'WW$ and $Z'Z'ZZ$ couplings do generate corrections to both T and S parameters. Such loop corrections are logarithmical divergent, and they lead to the renormalisation of the parameters β_1 and $\alpha_{1,8}$ in the EEWCL. Therefore, the new physics effects must be encoded in the renormalised value of those parameters, and no robust and model independent bound on the couplings of the Z' can be extracted. Furthermore, the allowed window for the coupling g_0 provides enough suppression to evade eventual bounds from the finite contribution of the loops. Another issue regards the discovery potential at the LHC: as the only tree level couplings at the order we are interested in

JHEP05(2014)088

involve heavy gauge bosons, the only channels where the Z' can be produced are production in association with a gauge boson ($pp \to Z'Z'(W,Z)$) and vector boson fusion production ($pp \to Z'Z'jj$). One may therefore look for a single W/Z signal or monojet. However, these channels suffer from large backgrounds, and we checked that the small allowed values of the couplings ($g_0 \sim 10^{-3}$–10^{-2}) would lead to cross sections that are too small to be detected at the LHC. We therefore conclude that the minimal model we study in this paper is not accessible at the LHC.

7 Summary

In this paper, we have investigated a rarely discussed possibility where a Z' boson is the sole DM candidate.
We considered an extended chiral Lagrangian with an additional U(1) gauge symmetry, with the following additional assumptions:

1. dark Z' is higgsphobic, i.e., it does not directly couple to the Higgs,
2. dark Z' is fermiophobic, i.e., it does not directly couple to SM fermions,
3. there is no CP violating Z' couplings,
4. there is no anomalous Z' couplings,
5. dark Z' does not mix with γ and the Z boson, and
6. there is no Z' interaction linear in the Z' field.

The remaining quartic vertices, $Z'Z'ZZ$ and $Z'Z'W^+W^-$, then dominate the Z' physics, which has four independent effective coupling constants g_1, g_2, g_3, g_4. We found that the mass of this dark Z' is not allowed below the W boson mass threshold, due to a combination of strong constraints from the relic density and those from direct-detection experiments. For mass $M_{Z'} > 100$GeV, from the relic density and direct and indirect-detection experiments where effective $Z'Z'q\bar{q}$ couplings are induced from SM gauge-boson loops, we produce five different coupling scenarios that are in the region 10^{-3}–10^{-2} (for the universal case, the result is given in figure 14). This range of coupling can be relaxed beyond the five cases analyzed for direct-detection experiments, but cannot be changed for indirect-detection experiments. To improve FermiLAT γ-ray spectra by our dark Z', we require a boost factor from 300 to 8000. We checked that even if our dark Z' mass lies within the low-energy region, it cannot reduce tensions among the observed possible DM signals with other null-result experiments. The bounds we extracted are therefore rather robust and model-independent.

Acknowledgments

This work was supported by the National Science Foundation of China (NSFC) under Grant No. 11075085, National Basic Research Program of China (973 Program) under Grant No. 2010CB833000, the Specialized Research Fund for the Doctoral Program of High Education

JHEP05(2014)088

of China No. 20110002110010, France China Particle Physics Laboratory (FCPPL) financial support, and the Tsinghua University Initiative Scientific Research Program. GC and AD also acknowledge partial support from the Labex-LIO (Lyon Institute of Origins) under grant ANR-10-LABX-66. AD is partially supported by Institut Universitaire de France.

A List of couplings

$$
\begin{aligned}
C_{\gamma-+} &= -\frac{g^3 g'}{g_Z}\left(\frac{1}{g^2}+\alpha_2+\alpha_3+\alpha_9\right)\\
C_{Z-+} &= -\frac{g^2}{g_Z}[1-g'^2\alpha_2+g^2(\alpha_3+\alpha_9)]\\
C_{Z'-+} &= -2g^2 g''\alpha_{31}\\
C_{+\gamma-} &= -\frac{gg'}{g_Z}\\
C_{+Z-} &= -\frac{g^2}{g_Z}-g^2 g_Z\alpha_3\\
C_{+Z'-} &= 0\\
C_{V_1V_2V_3} &= 0
\end{aligned}
\tag{A.1}
$$

Here, $g_Z \equiv \sqrt{g_0^2+g_1^2}$.

$$
\begin{aligned}
D_{++--} &= \frac{g^2}{2}+g^4\left(\alpha_3+\frac{\alpha_4}{2}+\alpha_9\right)\\
D_{+-+-} &= -\frac{g^2}{2}+g^4\left(-\alpha_3+\frac{\alpha_4}{2}+\alpha_5-\alpha_9\right)\\
D_{+-\gamma\gamma} &= -\frac{g^2 g'^2}{g_Z^2}\\
D_{+-ZZ} &= -\frac{g^4}{g_Z^2}-2g^4\alpha_3+g^2 g_Z^2(\alpha_5+\alpha_7)\\
D_{+-Z'Z'} &= 4g^2 g''^2(\alpha_5+\alpha_{21})\\
D_{+-\gamma Z} &= -\frac{2g^3 g'}{g_Z^2}-2g^3 g'\alpha_3\\
D_{+-\gamma Z'} &= 0\\
D_{+-ZZ'} &= -2g^2 g_Z g''\alpha_{16}\\
D_{+\gamma-\gamma} &= \frac{g^2 g'^2}{g_Z^2}\\
D_{+Z-Z} &= \frac{g^4}{g_Z^2}+2g^4\alpha_3+g^2 g_Z^2(\alpha_4+\alpha_6)\\
D_{+Z'-Z'} &= 4g^2 g''^2(\alpha_4+\alpha_{19})\\
D_{+\gamma-Z} &= \frac{g^3 g'}{g_Z^2}+g^3 g'\alpha_3\\
D_{+\gamma-Z'} &= D_{+Z'-\gamma}=0
\end{aligned}
$$

JHEP05(2014)088

$$
\begin{aligned}
D_{+Z-\gamma} &= D_{+\gamma-Z} = \frac{g^3 g'}{g_Z^2} + g^3 g' \alpha_3 \\
D_{+Z-Z'} &= D_{+Z'-Z} = -g^2 g_Z g'' \alpha_{17} \\
D_{ZZZZ} &= \frac{1}{4} g_Z^4 (\alpha_4 + \alpha_5 + 2\alpha_6 + 2\alpha_7 + 2\alpha_{10}) \\
D_{Z'ZZZ} &= -g_Z^3 g'' (2\alpha_{15} + \alpha_{16} + \alpha_{17}) \\
D_{Z'Z'ZZ} &= g''^2 g_Z^2 (\alpha_5 + 2\alpha_7 + 4\alpha_{20} + 2\alpha_{21}) \\
D_{Z'ZZ'Z} &= 4 g''^2 g_Z^2 (\alpha_4 + \alpha_6 + 2\alpha_{18} + \alpha_{19}) \\
D_{Z'Z'Z'Z} &= -4 g''^3 g_Z (\alpha_{16} + \alpha_{17} + 2\alpha_{22}) \\
D_{Z'Z'Z'Z'} &= 4 g''^4 (\alpha_4 + \alpha_5 + 2\alpha_{19} + 2\alpha_{21} + 4\alpha_{23})
\end{aligned}
$$

References

[1] V. Silveira and A. Zee, *Scalar phantoms*, *Phys. Lett.* **B 161** (1985) 136 [INSPIRE].

[2] C.P. Burgess, M. Pospelov and T. ter Veldhuis, *The minimal model of nonbaryonic dark matter: a singlet scalar*, *Nucl. Phys.* **B 619** (2001) 709 [hep-ph/0011335] [INSPIRE].

[3] W.-L. Guo, L.-M. Wang, Y.-L. Wu, Y.-F. Zhou and C. Zhuang, *Gauge-singlet dark matter in a left-right symmetric model with spontaneous CP-violation*, *Phys. Rev.* **D 79** (2009) 055015 [arXiv:0811.2556] [INSPIRE].

[4] X.-G. He, S.-Y. Ho, J. Tandean and H.-C. Tsai, *Scalar dark matter and Standard Model with four generations*, *Phys. Rev.* **D 82** (2010) 035016 [arXiv:1004.3464] [INSPIRE].

[5] X.-G. He and J. Tandean, *Hidden Higgs boson at the LHC and light dark matter searches*, *Phys. Rev.* **D 84** (2011) 075018 [arXiv:1109.1277] [INSPIRE].

[6] K. Cheung, Y.-L.S. Tsai, P.-Y. Tseng, T.-C. Yuan and A. Zee, *Global study of the simplest scalar phantom dark matter model*, *JCAP* **10** (2012) 042 [arXiv:1207.4930] [INSPIRE].

[7] J.M. Cline, K. Kainulainen, P. Scott and C. Weniger, *Update on scalar singlet dark matter*, *Phys. Rev.* **D 88** (2013) 055025 [arXiv:1306.4710] [INSPIRE].

[8] J.-M. Zheng et al., *Constraining the interaction strength between dark matter and visible matter: I. Fermionic dark matter*, *Nucl. Phys.* **B 854** (2012) 350 [arXiv:1012.2022] [INSPIRE].

[9] K. Cheung, P.-Y. Tseng, Y.-L.S. Tsai and T.-C. Yuan, *Global constraints on effective dark matter interactions: relic density, direct detection, indirect detection and collider*, *JCAP* **05** (2012) 001 [arXiv:1201.3402] [INSPIRE].

[10] B.W. Lee and S. Weinberg, *Cosmological lower bound on heavy neutrino masses*, *Phys. Rev. Lett.* **39** (1977) 165 [INSPIRE].

[11] J.S. Hagelin, G.L. Kane and S. Raby, *Perhaps scalar neutrinos are the lightest supersymmetric partners*, *Nucl. Phys.* **B 241** (1984) 638 [INSPIRE].

JHEP05(2014)088

[12] R. Ding and Y. Liao, *Spin 3/2 particle as a dark matter candidate: an effective field theory approach*, *JHEP* **04** (2012) 054 [arXiv:1201.0506] [INSPIRE].

[13] P. Langacker, *The physics of heavy Z' gauge bosons*, *Rev. Mod. Phys.* **81** (2009) 1199 [arXiv:0801.1345] [INSPIRE].

[14] P. Langacker, G. Paz, L.-T. Wang and I. Yavin, *Z'-mediated supersymmetry breaking*, *Phys. Rev. Lett.* **100** (2008) 041802 [arXiv:0710.1632] [INSPIRE].

[15] P. Langacker, *The physics of heavy Z' gauge bosons*, *Rev. Mod. Phys.* **81** (2009) 1199 [arXiv:0801.1345] [INSPIRE].

[16] E. Salvioni, G. Villadoro and F. Zwirner, *Minimal Z' models: present bounds and early LHC reach*, *JHEP* **11** (2009) 068 [arXiv:0909.1320] [INSPIRE].

[17] J. Kumar and J.D. Wells, *CERN LHC and ILC probes of hidden-sector gauge bosons*, *Phys. Rev.* **D 74** (2006) 115017 [hep-ph/0606183] [INSPIRE].

[18] M. Pospelov, A. Ritz and M.B. Voloshin, *Secluded WIMP dark matter*, *Phys. Lett.* **B 662** (2008) 53 [arXiv:0711.4866] [INSPIRE].

[19] M. Pospelov, *Secluded* U(1) *below the weak scale*, *Phys. Rev.* **D 80** (2009) 095002 [arXiv:0811.1030] [INSPIRE].

[20] E. Dudas, Y. Mambrini, S. Pokorski and A. Romagnoni, *(In)visible Z' and dark matter*, *JHEP* **08** (2009) 014 [arXiv:0904.1745] [INSPIRE].

[21] S. Khalil, H.-S. Lee and E. Ma, *Bound on Z' mass from CDMS II in the dark left-right gauge model II*, *Phys. Rev.* **D 81** (2010) 051702 [arXiv:1002.0692] [INSPIRE].

[22] B. Batell, *Dark discrete gauge symmetries*, *Phys. Rev.* **D 83** (2011) 035006 [arXiv:1007.0045] [INSPIRE].

[23] M.R. Buckley, D. Hooper and J.L. Rosner, *A leptophobic Z' and dark matter from grand unification*, *Phys. Lett.* **B 703** (2011) 343 [arXiv:1106.3583] [INSPIRE].

[24] M.T. Frandsen, F. Kahlhoefer, S. Sarkar and K. Schmidt-Hoberg, *Direct detection of dark matter in models with a light Z'*, *JHEP* **09** (2011) 128 [arXiv:1107.2118] [INSPIRE].

[25] P. Gondolo, P. Ko and Y. Omura, *Light dark matter in leptophobic Z' models*, *Phys. Rev.* **D 85** (2012) 035022 [arXiv:1106.0885] [INSPIRE].

[26] V. Barger, D. Marfatia and A. Peterson, *LHC and dark matter signals of Z' bosons*, *Phys. Rev.* **D 87** (2013) 015026 [arXiv:1206.6649] [INSPIRE].

[27] A. Alves, S. Profumo and F.S. Queiroz, *The dark Z' portal: direct, indirect and collider searches*, *JHEP* **04** (2014) 063 [arXiv:1312.5281] [INSPIRE].

[28] G. Arcadi, Y. Mambrini, M.H.G. Tytgat and B. Zaldivar, *Invisible Z' and dark matter: LHC vs LUX constraints*, *JHEP* **03** (2014) 134 [arXiv:1401.0221] [INSPIRE].

[29] B. Holdom, *Two* U(1)*'s and ϵ charge shifts*, *Phys. Lett.* **B 166** (1986) 196 [INSPIRE].

[30] B. Patt and F. Wilczek, *Higgs-field portal into hidden sectors*, hep-ph/0605188 [INSPIRE].

[31] T. Hambye, *Hidden vector dark matter*, *JHEP* **01** (2009) 028 [arXiv:0811.0172] [INSPIRE].

[32] G. Servant and T.M.P. Tait, *Is the lightest Kaluza-Klein particle a viable dark matter candidate?*, *Nucl. Phys.* **B 650** (2003) 391 [hep-ph/0206071] [INSPIRE].

JHEP05(2014)088

[33] H.-C. Cheng, J.L. Feng and K.T. Matchev, *Kaluza-Klein dark matter*, *Phys. Rev. Lett.* **89** (2002) 211301 [hep-ph/0207125] [INSPIRE].

[34] G. Bélanger, M. Kakizaki and A. Pukhov, *Dark matter in UED: the role of the second KK level*, *JCAP* **02** (2011) 009 [arXiv:1012.2577] [INSPIRE].

[35] B.A. Dobrescu, D. Hooper, K. Kong and R. Mahbubani, *Spinless photon dark matter from two universal extra dimensions*, *JCAP* **10** (2007) 012 [arXiv:0706.3409] [INSPIRE].

[36] G. Cacciapaglia, A. Deandrea and J. Llodra-Perez, *A dark matter candidate from Lorentz invariance in* 6*D*, *JHEP* **03** (2010) 083 [arXiv:0907.4993] [INSPIRE].

[37] A. Arbey, G. Cacciapaglia, A. Deandrea and B. Kubik, *Dark matter in a twisted bottle*, *JHEP* **01** (2013) 147 [arXiv:1210.0384] [INSPIRE].

[38] M. Frigerio, A. Pomarol, F. Riva and A. Urbano, *Composite scalar dark matter*, *JHEP* **07** (2012) 015 [arXiv:1204.2808] [INSPIRE].

[39] T.A. Ryttov and F. Sannino, *Ultra minimal technicolor and its dark matter TIMP*, *Phys. Rev.* **D 78** (2008) 115010 [arXiv:0809.0713] [INSPIRE].

[40] Y. Zhang, S.-Z. Wang and Q. Wang, *Stückelberg mechanism and chiral Lagrangian for* Z' *boson*, *JHEP* **03** (2008) 047 [arXiv:0803.1275] [INSPIRE].

[41] Q.-H. Cao, C.-R. Chen, C.S. Li and H. Zhang, *Effective dark matter model: relic density, CDMS II, Fermi LAT and LHC*, *JHEP* **08** (2011) 018 [arXiv:0912.4511] [INSPIRE].

[42] Z.-H. Yu et al., *Constraining the interaction strength between dark matter and visible matter: II. scalar, vector and spin-*3/2 *dark matter*, *Nucl. Phys.* **B 860** (2012) 115 [arXiv:1112.6052] [INSPIRE].

[43] T. Appelquist and G.-H. Wu, *The electroweak chiral Lagrangian and new precision measurements*, *Phys. Rev.* **D 48** (1993) 3235 [hep-ph/9304240] [INSPIRE].

[44] E.W. Kolb and M.S. Turner, *The early universe*, *Nature* **294** (1981) 521 [INSPIRE].

[45] PLANCK collaboration, P.A.R. Ade et al., *Planck* 2013 *results. XVI. Cosmological parameters*, arXiv:1303.5076 [INSPIRE].

[46] XENON100 collaboration, E. Aprile et al., *Dark matter results from* 225 *live days of XENON*100 *data*, *Phys. Rev. Lett.* **109** (2012) 181301 [arXiv:1207.5988] [INSPIRE].

[47] LUX collaboration, D.S. Akerib et al., *First results from the LUX dark matter experiment at the Sanford Underground Research Facility*, *Phys. Rev. Lett.* **112** (2014) 091303 [arXiv:1310.8214] [INSPIRE].

[48] SUPERCDMS collaboration, R. Agnese et al., *Search for low-mass WIMPs with SuperCDMS*, arXiv:1402.7137 [INSPIRE].

[49] PAMELA collaboration, O. Adriani et al., *PAMELA results on the cosmic-ray antiproton flux from* 60 *MeV to* 180 *GeV in kinetic energy*, *Phys. Rev. Lett.* **105** (2010) 121101 [arXiv:1007.0821] [INSPIRE].

[50] N. Fornengo, L. Maccione and A. Vittino, *Constraints on particle dark matter from cosmic-ray antiprotons*, *JCAP* **04** (2014) 003 [arXiv:1312.3579] [INSPIRE].

[51] AMS collaboration, M. Aguilar et al., *First result from the alpha magnetic spectrometer on the International Space Station: precision measurement of the positron fraction in primary cosmic rays of* 0.5–350 *GeV*, *Phys. Rev. Lett.* **110** (2013) 141102 [INSPIRE].

JHEP05(2014)088

[52] J. Kopp, *Constraints on dark matter annihilation from AMS-02 results*, *Phys. Rev.* **D 88** (2013) 076013 [arXiv:1304.1184] [INSPIRE].

[53] J.F. Navarro, C.S. Frenk and S.D.M. White, *A universal density profile from hierarchical clustering*, *Astrophys. J.* **490** (1997) 493 [astro-ph/9611107] [INSPIRE].

[54] L. Bergstrom, P. Ullio and J.H. Buckley, *Observability of gamma-rays from dark matter neutralino annihilations in the Milky Way halo*, *Astropart. Phys.* **9** (1998) 137 [astro-ph/9712318] [INSPIRE].

[55] FERMI-LAT collaboration, M. Ackermann et al., *Dark matter constraints from observations of 25 milky way satellite galaxies with the Fermi Large Area Telescope*, *Phys. Rev.* **D 89** (2014) 042001 [arXiv:1310.0828] [INSPIRE].

[56] J.L. Feng, J. Kumar, D. Marfatia and D. Sanford, *Isospin-violating dark matter*, *Phys. Lett.* **B 703** (2011) 124 [arXiv:1102.4331] [INSPIRE].

[57] M.I. Gresham and K.M. Zurek, *Light dark matter anomalies after LUX*, *Phys. Rev.* **D 89** (2014) 016017 [arXiv:1311.2082] [INSPIRE].

[58] V. Cirigliano, M.L. Graesser, G. Ovanesyan and I.M. Shoemaker, *Shining LUX on isospin-violating dark matter beyond leading order*, arXiv:1311.5886 [INSPIRE].

[59] E. Del Nobile, G.B. Gelmini, P. Gondolo and J.-H. Huh, *Update on light WIMP limits: LUX, lite and light*, *JCAP* **03** (2014) 014 [arXiv:1311.4247] [INSPIRE].

[60] CDMS collaboration, R. Agnese et al., *Silicon detector dark matter results from the final exposure of CDMS II*, *Phys. Rev. Lett.* **111** (2013) 251301 [arXiv:1304.4279] [INSPIRE].

[61] M.T. Frandsen and I.M. Shoemaker, *The up-shot of inelastic down-scattering at CDMS-Si*, arXiv:1401.0624 [INSPIRE].

[62] S.-Z. Wang, S.-Z. Jiang, F.-J. Ge and Q. Wang, *Electroweak chiral Lagrangian for W' boson*, *JHEP* **06** (2008) 107 [arXiv:0805.0643] [INSPIRE].

[63] E.J. Chun, J.-C. Park and S. Scopel, *Dark matter and a new gauge boson through kinetic mixing*, *JHEP* **02** (2011) 100 [arXiv:1011.3300] [INSPIRE].

JHEP05(2014)088